

**Theory of spin filtering through quantum dots**

J. Fransson,\* E. Holmström, and O. Eriksson

*Department of Physics, Uppsala University, Box 530, 751 21 Uppsala, Sweden*

I. Sandalov

*Department of Physics, Uppsala University, Box 530, 751 21 Uppsala, Sweden  
and Kirensky Institute of Physics, RAS, 660036 Krasnoyarsk, Russian Federation*

(Received 8 November 2002; revised manuscript received 4 February 2003; published 14 May 2003)

Using a nonequilibrium diagram technique for Hubbard operator Green functions combined with a generalization of the transfer Hamiltonian formalism, we calculate the transport through a magnetic quantum dot system with spin-dependent couplings to the contacts. In specific regimes of the parameter space the spin-dependent tunnel current becomes more than 99.95% spin polarized, suggesting that a device thus constructed can be used in spin-filter applications. First-principles electronic structure calculations show the existence of nanostructured systems, such as, e.g., MgO/Fe/Pd<sub>5</sub>/Fe/MgO (001), with the desired properties in the direction of the current.

DOI: 10.1103/PhysRevB.67.205310

PACS number(s): 72.25.-b, 73.63.Kv, 73.40.Gk

**I. INTRODUCTION**

Lately, there has been a substantial progress concerning spin-dependent tunneling,<sup>1-5</sup> magnetotransport,<sup>6-11</sup> and the possibility to apply these findings to devices. For instance, many suggestions of spin-filter devices<sup>12-17</sup> have been reported. In most of these reports, magnetic fields have been used to provide a spin current through the device, applied either directly over the device<sup>2-4,6-15</sup> or to polarize the contacts only.<sup>1,5,16</sup> In addition, by exploiting a combination of spin splitting of the resonant level induced by the Rashba effect and the spin-blockade phenomenon, it was proposed in Ref. 17 that a more than 99.9% spin-polarized current can be achieved in a triple-barrier resonant tunneling diode. Recently it has also been demonstrated that it is possible to fabricate nanodevices from a vast range of materials, with different characteristics, e.g., transport properties. Furthermore, theory has demonstrated the ability to reproduce many experimental results. Hence, in the search for novel devices, it becomes fruitful to augment experimental activities with theoretical work, where combinations of materials with unique properties can be predicted.

In this paper we suggest a structure that yields a nearly 100% spin-polarized current. For this purpose, we use a nonequilibrium many-body approach<sup>18,19</sup> in combination with a generalization of the transfer Hamiltonian formalism<sup>20-22</sup> to demonstrate a large spin dependence in the tunnel current through a magnetic quantum dot (QD). Technically this is achieved by letting the QD be coupled to the contacts with different tunneling probabilities for the spin channels and by having nondegenerate spin levels in the quantum dot region. The different tunneling probabilities are provided by tunnel barriers of different widths and/or heights for the two spin channels. Moreover, the spin-dependent couplings between the contacts and the QD generate a dramatic change in the population numbers of the localized levels. The combination of these effects leads to a strongly spin-polarized tunnel current through the system. The parameters used in our theoret-

ical model have been extracted from a first-principles calculation of a Fe/Pd nanolattice (a few atomic layers of Fe and Pd stacked on top of each other). The choice of a Fe/Pd<sub>5</sub>/Fe nanolattice is made since it is known to provide a large exchange splitting. Our results suggest that a device constructed in the described fashion, can be used in spin-filter applications.

**II. THEORETICAL MODEL**

The geometry considered here consists of metallic contacts that are tunnel coupled to a magnetic nanolattice, which we loosely will refer to as the QD region. One should bear in mind that a QD is a (quasi-)zero-dimensional object and our labeling of the here-suggested (quasi-)two-dimensional structure as a QD is not strictly correct. However, from a model point of view the transport through this heterostructure is identical to transport in a QD, which motivates our nomenclature. In between the QD region and the contacts there will be an insulating region that provides a potential barrier. An example of materials and geometry chosen for conducting an experiment relevant to our theoretical prediction is therefore the following: a metallic substrate followed by an insulating layer of MgO (NaCl structure in the 001 direction, lattice constant  $\sim 0.42$  nm) or similar insulating materials, the QD region (Fe/Pd<sub>5</sub>/Fe), followed by another layer of MgO that is followed by the second metallic contact. Adequate elements, that guarantees that the lattice mismatch is small, are Al, Ag, and Au as metal contacts. These elements also have a low resistivity, which is appropriate for our assumption of noninteracting metal contacts. The lattice mismatch is around 7% or less, which is technically manageable. The conductance is studied between the two metallic contacts and thus corresponds to a conductivity perpendicular to the plane (CPP).

Considering the transport properties of this system when being attached to external contacts, the investigation is undertaken in two different approaches. In the first approach,

we employ the single-electron picture by means of nonequilibrium Green functions (GF) and the overlap between the contacts and the QD taken into account. Here we consider electrons on the levels closest to (below)  $E_F$  as weakly interacting. In the second approach, the nonequilibrium many-body GF, we restrict the study to the two levels closest below  $E_F$ , taking into account kinematic interactions induced by the presence of the contacts.

When the electrons in the QD are weakly interacting, the total Hamiltonian for the system can be written

$$\mathcal{H} = \sum_{k\sigma \in L,R} \varepsilon_{k\sigma} c_{k\sigma}^\dagger c_{k\sigma} + \sum_{i \in \text{QD}} \varepsilon_i d_i^\dagger d_i + \sum_{k\sigma,i} (v_{k\sigma,i} c_{k\sigma}^\dagger d_i + \text{H.c.}). \quad (1)$$

Here  $c_{k\sigma}^\dagger$ , ( $c_{k\sigma}$ ) creates (annihilates) a conduction electron in the left ( $L$ ) or the right ( $R$ ) contact at the energy  $\varepsilon_{k\sigma}$ , whereas  $d_i^\dagger$  ( $d_i$ ) are the corresponding QD operators. The QD levels are calculated (see below) to be  $\varepsilon_i = -0.21$ ,  $-3.20$ , and  $-9.87$  meV: cf. Fig. 1. The transfer rate of electrons between the contacts and the QD is given by  $v_{k\sigma,i}$ .

Including the nonorthogonality between the states in the contacts and the QD alters the anticommutation relations between  $c_{k\sigma}$  and  $d_i^\dagger$  to<sup>20–22</sup>  $\{c_{k\sigma}, d_i^\dagger\} = \mathcal{O}_{k\sigma i}^{-1}$ , where  $\mathcal{O}_{k\sigma i}^{-1}$  is an element of the inverted overlap matrix which is defined by  $\mathcal{O}_{k\sigma i} = \langle k\sigma | i \rangle = \mathcal{O}_{ik\sigma}^*$ . Here  $|k\sigma\rangle$  and  $|i\rangle$  denote states in the contacts and QD, respectively. The spectral density  $\rho_i(\omega)$  for the  $i$ th level in the QD is thus given by the expression

$$\rho_i(\omega) = -\frac{1}{\pi} \text{Im} \frac{1 + v_\sigma^r(\omega)}{\omega - \varepsilon_i - \sum_{k \in L,R} \mathcal{O}_{ik\sigma}^{-1} v_{k\sigma,i} - V_\sigma^r(\omega)}, \quad (2)$$

where the effective interactions are defined by<sup>22</sup>

$$v_\sigma^r(\omega) = \sum_{k \in L,R} \frac{V_{i,k\sigma}^* \mathcal{O}_{k\sigma i}^{-1}}{\omega - \varepsilon_{k\sigma} + i\delta}, \quad (3)$$

$$V_\sigma^r(\omega) = \sum_{k \in L,R} \frac{V_{i,k\sigma}^* V_{k\sigma,i}}{\omega - \varepsilon_{k\sigma} + i\delta}. \quad (4)$$

Here we have used the notation  $V_{i,k\sigma} = v_{k\sigma,i} + \mathcal{O}_{k\sigma i}^{-1} \varepsilon_{k\sigma}$  and  $V_{k\sigma,i} = v_{k\sigma,i} + \mathcal{O}_{k\sigma i}^{-1} \varepsilon_i$ . The product  $V_{i,k\sigma} V_{k\sigma,i}$  reduces to  $|v_{k\sigma,i}|^2$  as the overlap  $\mathcal{O}_{k\sigma i}^{-1} \rightarrow 0$ , as expected.<sup>20–22</sup> Note, in Eq. (2), that the overlap induces a shift of the level which is of importance whenever the overlap between the contacts and the QD is large, i.e., when the tunnel barriers are either narrow and/or low.

The QD is assumed to be symmetrically coupled to the contacts. Thus the equilibrium conductance  $G = (dJ/d\Phi)|_{\Phi=0}$  (where  $\Phi$  is the bias voltage) through the  $i$ th level is calculated by the formula

$$G_i = \frac{e^2}{8k_B T \hbar} \int \Gamma_{\sigma,i}(\omega) \rho_i(\omega) \cosh^{-2} \left( \frac{\omega - \mu}{2k_B T} \right) d\omega, \quad (5)$$

where  $\Gamma_{\sigma,i}(\omega) = \Gamma_{\sigma,i}^L(\omega) \Gamma_{\sigma,i}^R(\omega) / [\Gamma_{\sigma,i}^L(\omega) + \Gamma_{\sigma,i}^R(\omega)]$ , the couplings  $\Gamma_{\sigma,i}^\alpha(\omega) = 2\pi \sum_{k \in \alpha} |V_{k\sigma,i}|^2 \delta(\omega - \varepsilon_{k\sigma})$ ,  $\alpha = L, R$  such that  $\Gamma_{\sigma,i}^L(\omega) = \Gamma_{\sigma,i}^R(\omega)$ , and  $\mu$  is the equilibrium chemical potential.

### III. CALCULATIONS OF PARAMETERS

Next, we describe briefly how the electronic structure of the QD was calculated and discuss the result. From first-principles density functional calculations (described below) we have found that a two-dimensional layered system in equilibrium, consisting of vac/Fe/Pd<sub>5</sub>/Fe/vac, exhibits desired properties in the direction perpendicular to the interface. It should be noted here that an experimental geometry is not thought to consist of free standing Fe/Pd<sub>5</sub>/Fe layers (an impossible experimental situation), but of, e.g., MgO/Fe/Pd<sub>5</sub>/Fe/MgO. Due to the large band gap in the MgO (or similar material) layer, there is very little influence on the electronic structure of the Fe and Pd atoms, and simulating the electronic structure of such a multilayer by considering vac/Fe/Pd<sub>5</sub>/Fe/vac has been shown to be a good approximation.<sup>23</sup> The electronic structure of the nanolayer was calculated by means of the full potential linear muffin tin orbital method.<sup>24</sup> The system consisted of a five-monolayer-(ML-) thick Pd slab sandwiched between 1-ML-thick Fe layers together with an 1.17-nm-thick vacuum barrier (the Fe-Fe distance in the repeated supercell). The system was assumed to grow in the fcc (001) direction with perfect interfaces and without relaxation. The lattice parameter was the same as for bulk Pd (0.389 nm). Care was taken to converge the calculations with respect to  $\mathbf{k}$ -point sampling, basis set truncation, and the self-consistency criterion. In addition, we used the local density approximation in the parametrization of von Barth and Hedin, and all relativistic effects were included.

As concerns the basic magnetic structure of the Fe/Pd slab, we find a strong magnetic polarization at the Fe atoms with a magnetic moment inside the muffin tin sphere of  $3.08\mu_B$ . The polarization of the Pd atoms is also not negligible, and we find that the Pd atom closest to the Fe/Pd interface has a magnetic moment of  $0.20\mu_B$  parallel to the Fe moment, while the other Pd atoms show only a very small magnetic polarization. The total magnetic moment of the multilayer is  $6.82\mu_B$ /f.u. (formula unit).

We proceed by extracting effective parameters from our electronic structure calculation, used in the expressions for the conductance through the QD. Thus we need the eigenvalues of the electron states within the Fe/Pd nanolattice, as well as heights and widths of the tunnel barriers between the contacts and QD [for the calculations using Eq. (5)]. The former is straightforward, since it is the outcome of our first-principles calculation. The calculated eigenvalues of the system in the energy range  $-10$  to  $+15$  meV around  $E_F$  are drawn in Fig. 1. Since we consider only bias voltages less than 20 mV, the three states below  $E_F$  in Fig. 1 are the only ones that significantly contribute to the current through the QD. It should be noted that the calculation of transport properties was made assuming a square well model potential, for the conducting electron states; see Fig. 2. A sensible way of

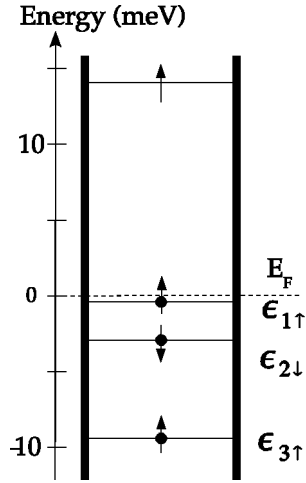


FIG. 1. Eigenvalues corresponding to eigenstates with overlapping spectral density through the vacuum region. The energies of the states are (from the top) 13.61,  $-0.21$ ,  $-3.20$ , and  $-9.87$  meV, respectively. The arrows indicate the spin direction with the largest probability for each state. States above  $E_F$  are unoccupied.

estimating the barrier height is from the band gap of the insulating layer between the leads and QD. Since the present work outlines a general methodology, without being materials specific for the insulating layer, we have used a typical band-gap value of  $\sim 1$  eV.

It remains to find the widths of the barriers in Fig. 2. To extract the width of the barriers we focus our attention to the wave functions (or rather electron density) of the eigenvalues in Fig. 1. In Fig. 3 we show the density (both spin up and spin down) in the  $zx$  plane, for the eigenstate just below  $E_F$ , where  $z$  is the direction perpendicular to the interface. We remark here that the only reason this state (which in Fig. 1

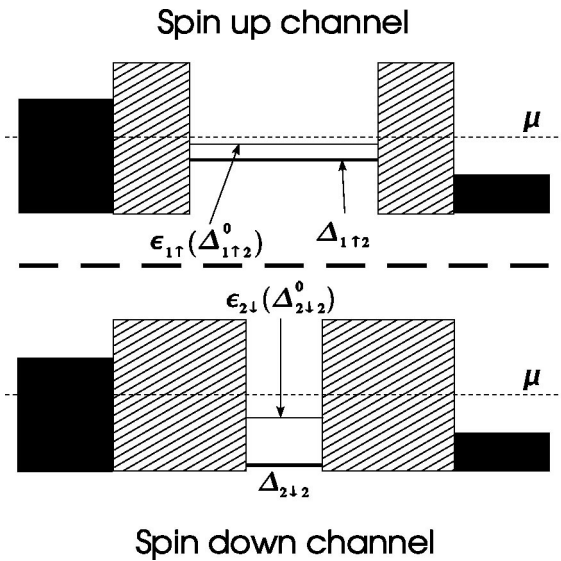


FIG. 2. Model potentials for the spin  $\uparrow$  and  $\downarrow$  channels, respectively. The energy levels  $\epsilon_{1\uparrow}$  and  $\epsilon_{2\downarrow}$  represent the two levels closest below  $E_F$  in Fig. 1. The transition energies  $\Delta_{1\uparrow 2}$  ( $\Delta_{1\uparrow 2}^0$ ) and  $\Delta_{2\downarrow 2}$  ( $\Delta_{2\downarrow 2}^0$ ) correspond to the dressed (bare) transitions discussed in Sec. V.

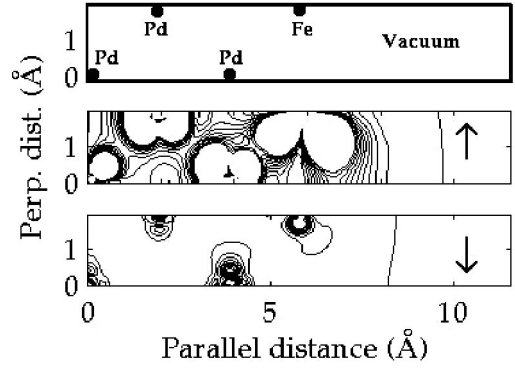


FIG. 3. The density for the eigenstate with energy  $-0.21$  meV in the  $zx$  plane in the fcc (100) direction. The direction labeled parallel is along the direction of the current. Arrows indicate the spin direction. The upper panel shows schematically the positions of the Pd and Fe atoms.

schematically is marked as spin up) has both spin-up and spin-down character is that we included the spin-orbit coupling in our calculation, which mixes the two spin components. Typically an electron state inside the QD has a wave function admixture such that its charge density has a combination of  $\sim 90\%$  for one spin channel and  $\sim 10\%$  for the other. It is clearly seen in Fig. 3 that the distributions of the densities for the two spin channels are very different. For the spin-up projection the state is evenly distributed over the metal region of the system with a large weight on the Fe atom at the interface. For the spin-down projection the weight is smaller and mostly localized on the atoms and, in particular, the distribution around the Fe atom is very different. By investigating the density around the Fe atom in more detail we find that the density for both the spin-up and spin-down cases shows an exponential decrease into the vacuum region, as expected. However, the behavior is very different between the two spin channels. This finding is not too surprising, and it holds for all eigenstates shown in Fig. 1. A consequence drawn from this observation is, however, that different eigenvalues will experience different tunneling matrix elements. In order to simulate this behavior in our model potential (Fig. 2) we define the widths of the spin-up and spin-down barriers by a critical value of the amplitude of the wave function (or, rather, the electron density). Hence we define a critical value for the intensity of the electron density as  $7.6 \times 10^{-7}$  electrons/(a.u.),<sup>3</sup> corresponding to the orbital density, which in this region and outwards from the center of the heterostructure is exponentially decaying, being negligible compared to its maximum. With this criterion, we find that, e.g., for the highest occupied state in Fig. 1, the spin-up channel reaches the critical value a distance 0.97 nm from the center Pd atom. The spin-down channel reaches the same value at 0.85 nm, and in this way we estimate different effective tunnel barriers for each particular state, i.e., 0.7809 nm (0.9009 nm) for the spin- $\uparrow$  ( $\downarrow$ ) channel. Since the spin- $\downarrow$  probability of this eigenvalue is at most 10% and the barrier thickness is sufficiently large, we have neglected the spin- $\downarrow$  contribution from this state. The other two states have been treated analogously. The calculated barrier widths are found to be quite insensitive with respect to the choice of critical

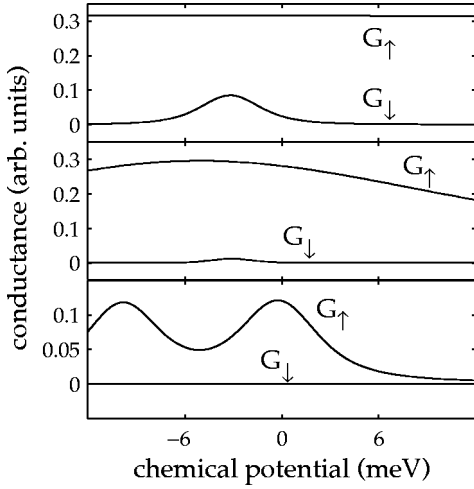


FIG. 4. The total conductance for each spin projection (two levels with spin  $\uparrow$  and one with spin  $\downarrow$ ) for three different widths of the tunnel barriers as a function of  $\mu$ . In the upper panel the widths are [0.7809, 0.9899, 0.7925] nm, corresponding to the eigenvalues  $[-0.21, -3.20, -9.87]$  meV: in the middle and lower panels the widths 0.3174 and 0.5819 nm, respectively, have been added to the original widths, thus extending the distance between the contacts and QD. Calculations are performed with barrier heights  $\sim 1$  eV, conduction electrons band width  $2W \sim 4.40$  eV at  $T = 10$  K.

value of the electron density. Changing the value of the critical electron density with 100% gives a negligible modification of the barrier widths.

#### IV. CALCULATIONS OF TRANSPORT PROPERTIES

With the parameters calculated in the previous section, the total conductance for each spin projection (two levels with spin  $\uparrow$  and one with spin  $\downarrow$ ) is plotted in Fig. 4 for three different widths of the tunnel barriers as a function of the chemical potential  $\mu$ , which is common in the whole system since other external fields are absent. Experimentally  $\mu$  can be varied, for example, by applying a gate voltage over the interface structure. In the first case, Fig. 4 (upper panel), we use widths of the tunnel barriers found from the calculations on the vac/Fe/Pd/Fe/vac structure. It is seen that the conductance in the spin- $\uparrow$  channel dominates the transport. Actually, calculations of the current show that the spin- $\downarrow$  current is less than 11% for bias voltages less than 20 mV. This is clear since the overlap between the spin- $\downarrow$  states in the contacts and QD level  $\epsilon_{2\downarrow}$  (see Fig. 1) is much smaller than the corresponding overlaps to  $\epsilon_{i\uparrow}$ ,  $i=1,3$ , due to the large barrier widths in the spin- $\downarrow$  channel. By increasing the distance between the contacts and QD, Fig. 4 (middle and lower panels), thus making the overlaps smaller, the conductance of the spin- $\downarrow$  channel is seen to decrease substantially. The corresponding calculations of the currents shows that the contribution from the spin- $\downarrow$  current is less than 1.5% (middle panel) and 0.052% (lower panel), respectively. The obvious conclusion, then, is that the layered structure can be used as a spin filter if the distance between the contacts and QD is sufficiently large to provide a negligible overlap in the spin- $\downarrow$

channel—however, sufficiently small to preserve an observable conductance in the spin- $\uparrow$  channel.

#### V. EFFECTS OF ELECTRON CORRELATIONS

In the second approach considered here, we include correlations between the electrons. For simplicity, we restrict the further discussion to the two levels closest below  $E_F$ : see Fig. 1. By treating these levels as the energies of transitions between many-electron states, we can include kinematic interactions of the levels induced by the conduction electrons in the contacts. In modeling the QD, we start by disconnecting the contacts and map the results from the first-principles calculations to the Kanamori model<sup>25</sup> with four orbitals, i.e.,

$$\mathcal{H} = \sum_{\sigma} (\epsilon_1 n_{1\sigma} + \epsilon_2 n_{2\sigma}) + U_1 n_{1\uparrow} n_{1\downarrow} + U_2 n_{2\uparrow} n_{2\downarrow} + U_{12} (n_{1\uparrow} + n_{1\downarrow})(n_{2\uparrow} + n_{2\downarrow}) - \frac{J}{2} (n_{1\uparrow} n_{2\uparrow} + n_{1\downarrow} n_{2\downarrow}). \quad (6)$$

Here the second and third terms describe the Coulomb repulsion within the same orbital, where  $n_{i\sigma} = d_{i\sigma}^\dagger d_{i\sigma}$ , and the fourth and fifth terms give the Coulomb and exchange interactions between the orbitals, respectively. As discussed below, the admixture of the spin- $\uparrow$  and  $\downarrow$  orbitals due to the spin-orbit coupling is small and is, therefore, neglected. It is known<sup>26</sup> that  $U_i > U_{12}$  and by putting  $U_1 = U_2 = U$ , which is reasonable for the localized orbitals, we find that

$$E_{1\uparrow} = \epsilon_1 + 2U_{12} - J/2, \quad E_{1\downarrow} = E_{1\uparrow} + U_2,$$

$$E_{2\downarrow} = \epsilon_2 + U + U_{12}, \quad E_{2\uparrow} = E_{2\downarrow} - J/2,$$

with the constraints that  $\langle n_{1\uparrow} \rangle = \langle n_{2\downarrow} \rangle = \langle n_{2\uparrow} \rangle = 1$  ( $\langle n_{1\downarrow} \rangle = 0$ ). Thus, by requiring the spin  $\downarrow$  and  $\uparrow$  states for the first and second orbitals to be far above and below  $E_F$ , respectively, we can map the other two levels onto the calculations on the layered Fe/Pd heterostructure. Hence  $E_{1\uparrow} = -0.21$  meV and  $E_{2\downarrow} = -3.20$  meV.

In principle, when a bias voltage is applied to the system, there will be transitions between the two-, one-, and zero-particle states. However, the energy of any transition to the empty state is large and can be neglected. The treatise is now reduced to involve only two transitions and the diagonal Hamiltonian for the QD can be written  $\mathcal{H}_{\text{QD}} = \sum_p E_p X^{pp}$ , where  $X^{pq} = |p\rangle\langle q|$  is a Hubbard operator<sup>27</sup> and  $p \in \{\uparrow, \downarrow, 2\}$ . Here  $|\sigma\rangle = \delta_{\sigma\uparrow} |\uparrow\rangle_1 |0\rangle_2 + \delta_{\sigma\downarrow} |0\rangle_1 |\downarrow\rangle_2$  and  $|2\rangle = |\uparrow\rangle_1 |\downarrow\rangle_2$ . The spectral density  $\rho_{\sigma}(\omega) = -\text{Im} G'_{\sigma}(\omega)/\pi$  where  $G_{\sigma}(t, t') = (-i) \langle T X^{2\sigma}(t) X^{\sigma'2}(t') \rangle / (TS)$ .<sup>5,18,19,22</sup>

In the time-independent regime the total spectral density for the two transitions involved is given by

$$\rho(\omega) = -\frac{1}{\pi} \text{Im} \sum_{\sigma} \frac{P'_{\sigma}(\omega)}{\omega - \Delta_{\sigma 2} - V'_{\sigma}(\omega) P'_{\sigma}(\omega)}. \quad (7)$$

The end factor  $P_{\sigma}(i\omega) = [1 + v_{\sigma}(i\omega) P_{\sigma}] P_{\sigma}$  is the dressed spectral weight where  $P_{\sigma} = N_2 + N_{\sigma}$  is the sum of the population numbers for the states  $|2\rangle$  and  $|\sigma\rangle$ , respectively, satis-

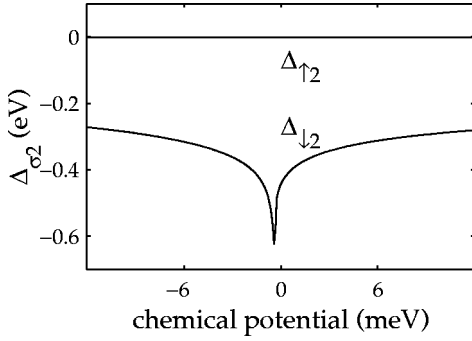


FIG. 5. The transition energies  $\Delta_{\uparrow 2}$  and  $\Delta_{\downarrow 2}$  as functions of the gate voltage. In the given gate voltage interval the transition energy  $\Delta_{\uparrow 1} \in \{-0.58, -0.40\}$  meV. The bare transitions are  $\Delta_{\uparrow 2}^0 = -0.21$  meV and  $\Delta_{\downarrow 2}^0 = -3.20$  meV. Other parameters correspond to the case in Fig. 4 (upper panel).

fying  $N_{\uparrow} + N_{\downarrow} + N_2 = 1$ . The population numbers  $N_{\sigma} = \text{Im} \int G_{\sigma}^<(\omega) d\omega / 2\pi$ , where formally  $G^< = G^r V^< G^a + D^r (P^< + P^< V^a G^a)$  with the locator  $D$  defined by  $G = D P$ .

In Eq. (7), the dressed transition energy  $\Delta_{\sigma 2} = \Delta_{\sigma 2}^0 + \delta\Delta_{\sigma 2} + \sum_{k \in L, R} \mathcal{O}_{ik\sigma}^{-1} V_{k\sigma, i}$ , where the bare transition energy  $\Delta_{\sigma 2}^0 = E_{i\sigma} - E_2$  and  $E_2 = 0$ . The index  $i$  denotes the relevant transition with spin  $\sigma$ . The last term in the expression for  $\Delta_{\sigma 2}$  corresponds to a similar contribution as in Eq. (2), whereas<sup>5,22</sup>

$$\delta\Delta_{\sigma 2} = \sum_{k \in L, R} V_{i, k\bar{\sigma}}^* V_{k\bar{\sigma}, i} \frac{f(\varepsilon_{k\bar{\sigma}}) - f(\Delta_{\bar{\sigma} 2})}{\varepsilon_{k\bar{\sigma}} - \Delta_{\bar{\sigma} 2}} \quad (8)$$

gives a correction from kinematic interactions, due to the presence of the contacts. It should be noticed that the transition energy for the spin- $\sigma$  channel strongly depends on the conduction properties in the opposite spin ( $\bar{\sigma}$ ) channel. Therefore, if the overlap in the spin  $\sigma$  channel is larger than that of the spin  $\bar{\sigma}$ , then  $\Delta_{\bar{\sigma} 2}$  is pushed further below  $\mu$  than what  $\Delta_{\sigma 2}$  is. This fact is effectively illustrated in Figs. 5 and 2, where  $\sigma = \uparrow$  and  $\bar{\sigma} = \downarrow$ . Actually, for small bias voltages the transition is pushed out of resonance. Thereto, the width of the corresponding transition is a very small,  $\delta$ -function-like peak in the spectral density.

In Fig. 5 it is seen that the transition  $\Delta_{\downarrow 2}$  has a sharp dip when  $\mu$  is in the vicinity of the transition  $\Delta_{\uparrow 2}$ . This is easily understood from Eq. (8), since when  $|\varepsilon_{k\uparrow} - \Delta_{\uparrow 2}| \rightarrow 0$  the renormalization  $\delta\Delta_{\downarrow 2} \rightarrow -\infty$ , implying that  $\Delta_{\downarrow 2}$  becomes increasingly shifted below  $\mu$ . Similarly, the transition  $\Delta_{\uparrow 2}$  diverges as  $|\varepsilon_{k\downarrow} - \Delta_{\downarrow 2}| \rightarrow 0$ . However, since the tunneling probability for the spin-down channel (reflected in the matrix elements  $V_{i, k\downarrow}^*$  and  $V_{k\downarrow, i}$ ) is substantially smaller than that for the spin-up channel, the renormalization becomes less apparent and is not seen in the large scale in Fig. 5.

The conductance for the two spin channels have been calculated within the formulation given in Eq. (5), however, modified to suit the present case with many-body transitions in the local density of states of the QD. Thus the contribution from the transition  $\Delta_{\downarrow 2}$  to the total conductance is less than 0.005%, leading to a very strong spin polarization of the

current through the system. In the given interval of the chemical potential the conductance appears without structures and is, therefore, not shown here.

## VI. DISCUSSION AND CONCLUSIONS

In our calculation of the current through the QD we have made several approximations. The calculated eigenvalue spectrum, shown in Fig. 1, is obtained for a uniform mesh of  $10 \times 10 \times 2$  ( $k_x, k_y, k_z$ )  $\mathbf{k}$  points of the QD region. Out of these  $\mathbf{k}$  points only three have eigenvalues in the vicinity of  $E_F$ : having a significant contribution to the conductivity, these eigenvalues are shown in Fig. 1. However, a larger number of  $\mathbf{k}$  points would possibly result in more levels lying within the energy region given by the considered bias voltage. Hence, the current must be calculated from a sum of such states in Eq. (2). In order to extract a very accurate number of the current, one must hence perform such a calculation for increasingly dense  $\mathbf{k}$ -point meshes, until one has reached convergence. However, our first-principles calculation shows that a dense  $\mathbf{k}$ -point sampling does not bring in any spin-down states close to the Fermi level since there is a gap (or at least pseudogap) in the spin-down density of states at the Fermi level.

Another approximation made here is to simulate the effective potential of the conducting electron state using a square well potential, with effective widths adjusted to the asymptotic part of the self-consistently calculated electron density. In addition we have assumed atomistically sharp interfaces between the Fe and Pd layers, which in an experimental situation should be replaced with alloy layers, some with dominant Fe concentration and other layers with dominant Pd concentration. Having these approximations in mind one should expect small deviations between experimental and our theoretical data, although we expect that the general trend as given by our theory should hold.

The highly spin-polarized current obtained within the two models for transport calculations can, of course, happen to be too optimistic. Actually there are two main mechanisms which can change the degree of spin polarization of the current: (i) spin-orbit coupling and (ii) spin waves in the magnetic sublayer (Fe in our case). The spin-orbit coupling is in itself acting in three ways: namely, (1) it changes the coupling between the metal contacts and the QD, (2) it mixes the spin components of the QD wave functions, and (3) it causes a magnetocrystalline anisotropy. The latter usually provides a gap in spin-wave spectrum and, therefore, at sufficiently small temperature and bias voltage the decrease of polarization due to these mechanism is exponentially small.

The admixture of spin-up and spin-down components of the wave function is  $\sim 11\%$ , as found from the first-principles calculations. As discussed above, this admixture should not change our results since the barrier for the spin-down component is thick (see Fig. 3) and, therefore, this component does not contribute to the current. The first mechanism, however, remains to be investigated.

To summarize, we have demonstrated that the tunnel current through a layered magnetic nanostructure, e.g., a  $\text{vac}/\text{Fe}/\text{Pd}_5/\text{Fe}/\text{vac}$  interface, coupled to external contacts via tunnel barriers with spin-dependent widths in some cases

shows a more than 99.95% spin polarization. Calculations performed both within single-particle and many-body approaches reveal the high degree of spin polarization of the current. We expect that a system thus constructed can be used as a static spin-filter device.

### ACKNOWLEDGMENTS

We acknowledge support from the Göran Gustafsson foundation, the Swedish National Research Council (VR), and the Swedish Foundation for Strategic Research (SSF).

\*Electronic address: Jonas.Fransson@fysik.uu.se

<sup>1</sup>M. Johnson, Phys. Rev. B **58**, 9635 (1998).

<sup>2</sup>M. Sharma, J. H. Nickel, T. C. Anthony, and S. X. Wang, Appl. Phys. Lett. **77**, 2219 (2000).

<sup>3</sup>Z. Li, C. de Groot, and J. H. Moodera, Appl. Phys. Lett. **77**, 3630 (2000).

<sup>4</sup>J. Wang, P. P. Freitas, and E. Snoeck, Appl. Phys. Lett. **79**, 4553 (2001).

<sup>5</sup>J. Fransson, O. Eriksson, and I. Sandalov, Phys. Rev. Lett. **88**, 226601 (2002).

<sup>6</sup>M. Julliere, Phys. Lett. **54A**, 225 (1975).

<sup>7</sup>J. S. Moodera, L. R. Kinder, T. M. Wong, and R. Meservey, Phys. Rev. Lett. **74**, 3273 (1995).

<sup>8</sup>J. C. Egues, Phys. Rev. Lett. **80**, 4578 (1998).

<sup>9</sup>M. Sharma, S. X. Wang, and J. H. Nickel, Phys. Rev. Lett. **82**, 616 (1999).

<sup>10</sup>T. Hayashi, M. Tanaka, and A. Asamitsu, J. Appl. Phys. **87**, 4673 (2000).

<sup>11</sup>H.-S. Sim, G. Ihm, N. Kim, and K. J. Chang, Phys. Rev. Lett. **87**, 146601 (2001).

<sup>12</sup>M. J. Gilbert and J. P. Bird, Appl. Phys. Lett. **77**, 1050 (2000).

<sup>13</sup>P. Recher, E. V. Sukhorukov, and D. Loss, Phys. Rev. Lett. **85**, 1962 (2000).

<sup>14</sup>G. Papp and F. M. Peeters, Appl. Phys. Lett. **78**, 2184 (2001).

<sup>15</sup>J. C. Egues, C. Gould, G. Richter, and L. W. Molenkamp, Phys. Rev. B **64**, 195319 (2001).

<sup>16</sup>A. L. Efros, M. Rosen, and E. I. Rashba, Phys. Rev. Lett. **87**, 206601 (2001).

<sup>17</sup>T. Koga, J. Nitta, H. Takayanagi, and S. Datta, Phys. Rev. Lett. **88**, 126601 (2002).

<sup>18</sup>I. Sandalov, B. Johansson, and O. Eriksson, cond-mat/0011259 (unpublished).

<sup>19</sup>I. Sandalov, U. Lundin, and O. Eriksson, cond-mat/0011260 (unpublished).

<sup>20</sup>J. Fransson, O. Eriksson, B. Johansson, and I. Sandalov, Physica B **272**, 28 (1999).

<sup>21</sup>J. Fransson, O. Eriksson, and I. Sandalov, Phys. Rev. B **64**, 153403 (2001).

<sup>22</sup>J. Fransson, O. Eriksson, and I. Sandalov, Phys. Rev. B **66**, 195319 (2002).

<sup>23</sup>C. Li and A. J. Freeman, Phys. Rev. B **43**, 780 (1991).

<sup>24</sup>J. M. Wills, O. Eriksson, and M. Alouani, in *Electronic Structure and Physical Properties of Solids*, edited by Hugues Dreyse (Springer-Verlag, Berlin, 2000), p. 148.

<sup>25</sup>J. Kanamori, Prog. Theor. Phys. Jpn. **30**, 275 (1963).

<sup>26</sup>I. S. Sandalov, O. Hjortstam, B. Johansson, and O. Eriksson, Phys. Rev. B **51**, 13 987 (1995).

<sup>27</sup>J. Hubbard, Proc. R. Soc. London, Ser. A **276**, 238 (1963); **277**, 237 (1963).